mpi
I N F O R M A T I K

Linear One-sided Stability of
MAT for Weakly Injective Domain

Sung Woo Choi and Hans-Peter Seidel

MPI–I–2001–4–004 June 2001

FORSCHUNGSBERICHT   RESEARCH REPORT

M A X - P L A N C K - I N S T I T U T
F Ü R
I N F O R M A T I K

Stuhlsatzenhausweg 85   66123 Saarbrücken   Germany

Author's Address

Sung Woo Choi and Hans-Peter Seidel
Computer Graphics Group
Max-Planck-Institut für Informatik
Stuhlsatzenhausweg 85, 66123 Saarbrücken, Germany
Email: {swchoi,hpseidel}@mpi-sb.mpg.de

Abstract

Medial axis transform (MAT) is very sensitive to the noise, in the sense that, even if a shape is perturbed only slightly, the Hausdorff distance between the MATs of the original shape and the perturbed one may be large. But it turns out that MAT is stable, if we view this phenomenon with the one-sided Hausdorff distance, rather than with the two-sided Hausdorff distance. In this paper, we show that, if the original domain is weakly injective, which means that the MAT of the domain has no end point which is the center of an inscribed circle osculating the boundary at only one point, the one-sided Hausdorff distance of the original domain's MAT with respect to that of the perturbed one is bounded linearly with the Hausdorff distance of the perturbation. We also show by example that the linearity of this bound cannot be achieved for the domains which are not weakly injective. In particular, these results apply to the domains with the sharp corners, which were excluded in the past. One consequence of these results is that we can clarify theoretically the notion of extracting "the essential part of the MAT", which is the heart of the existing pruning methods.

Keywords

1   Introduction

The *medial axis* (**MA**) of a plane domain is defined as the set of the centers of the maximal inscribed circles contained in the given domain. The *medial axis transform* (**MAT**) is defined as the set of all the pairs of the medial axis point and the radius of the corresponding inscribed circle. Because of the additional radius information, **MAT** can be used to reconstruct the original domain. More explicitly, the medial axis transform **MAT**(Ω) and the medial axis **MA**(Ω) of a plane domain Ω is defined by

$$\mathbf{MAT}(\Omega) = \{ (p, r) \in \mathbb{R}^2 \times [0, \infty) \,|$$
$$B_r(p) \text{ is a maximal ball contained in } \Omega \},$$

$$\mathbf{MA}(\Omega) = \{ p \in \mathbb{R}^2 \,|\, \exists r \geq 0, \text{ s.t. } (p, r) \in \mathbf{MAT}(\Omega) \}.$$

Medial axis (transform) is one of the most widely-used tools in shape analysis. It has a natural definition, and has a graph structure which preserves the original shape homotopically [2, 3].

But the medial axis transform has one weak point; It is not stable under the perturbation of the domain [9, 4, 1]. See Figure 1. Even when the domain on the left (a) is slightly perturbed to the domain on the right (b) (that is, the Hausdorff distance between the domains in (a) and (b) is small), the **MAT** (**MA**) changes drastically, which results in a large value of the Hausdorff distance between the **MAT**s (**MA**s) of the domains in (a) and (b).

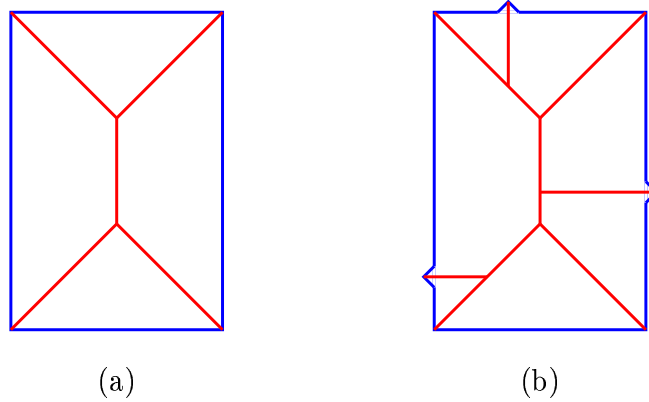(a)   (b)

Figure 1: Instability of **MAT**: Although a small perturbation of the domain may lead to a drastic change of the **MAT** (**MA**) in the (two-sided) Hausdorff distance, the one-sided Hausdorff distance still remains small.

This seemingly unplausible phenomenon can produce a lot of problems, especially in the recognition fields, since the data representing the domains

have inevitable noises. So there has been many attempts to reduce the complexity of the **MAT** by "pruning" out what is considered less important, or considered to be caused by the noise [8, 10, 6].

One important observation that can be made from Figure 1 is that the **MAT** (**MA**) in (a) is contained approximately in the **MAT** (**MA**) in (b). In other words, although the two-sided Hausdorff distance of the **MAT**s in (a) and (b) is large, the *one-sided* Hausdorff of the **MAT** in (a) with respect to that in (b) is still small.

In this paper, we analyze this phenomenon, and show that **MA** and **MAT** are indeed stable, if we measure the change by the one-sided Hausdorff distance instead of the two-sided Hausdorff distance. We will prove that, when a plane domain Ω satisfies a certain smoothness condition which we call the *weak-injectivity*, then the one-sided Hausdorff distance of $\mathbf{MA}(\Omega)$ (*resp.*, $\mathbf{MAT}(\Omega)$) with respect to $\mathbf{MA}(\Omega')$ (*resp.*, $\mathbf{MAT}(\Omega')$) has an upper bound which is *linear* with the Hausdorff distances between Ω, Ω' and between $\partial\Omega$, $\partial\Omega'$ for arbitrary domain Ω'. In particular, the weak-injectivity is shown to be essential for having the linear bound. This result extends the previous one for the *injective* domains [4]; We now can allow the sharp corners in the domains for which the linear one-sided stability is valid.

It turns out that the coefficient of the linear bound grows as the angle θ_Ω (See Section 2) characteristic to a weakly injective domain Ω decreases. An important consequence of this is that we can approximately measure the degree of the "detailed-ness" of a domain Ω by the value θ_Ω. Along with this, we will discuss about the relation between our result and the pruning of **MAT**.

2 Preliminaries

2.1 Normal Domains

Contrary to the common belief, $\mathbf{MAT}(\Omega)$ and $\mathbf{MA}(\Omega)$ may not be graphs with finite structure, unless the original domain Ω satisfies the following rather strong conditions [3]:

- Ω is compact, or equivalently, Ω is closed and bounded.

- The boundary $\partial\Omega$ of Ω is a (disjoint) union of finite number of simple closed curves, each of which in turn consists of finite number of real-analytic curve pieces.

So we will consider only the domains satisfying these conditions, which we call *normal*.
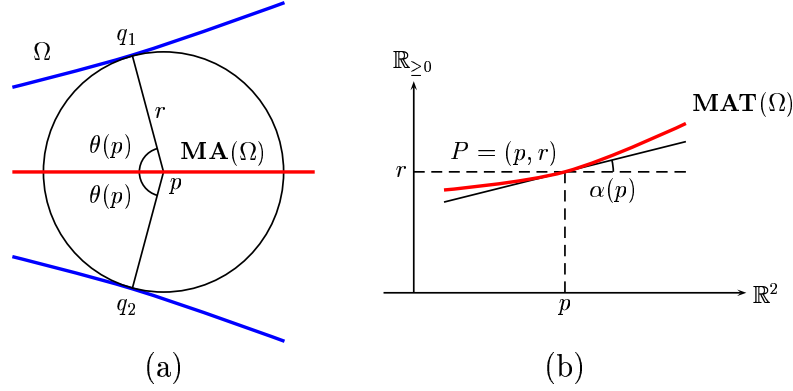
(a)   (b)

Figure 2: Local geometry of **MA** and **MAT** around a generic point

Let Ω be a normal domain. Then, except for some finite number of the special points, the maximal ball $B_r(p)$ for every $P = (p, r) \in \mathbf{MAT}(\Omega)$ has exactly two contact points with the boundary $\partial\Omega$. It is well known that $\mathbf{MA}(\Omega)$ (*resp.*, $\mathbf{MAT}(\Omega)$) is a C^1 curve around such p in $\mathbb{R}^2$ (*resp.*, P in $\mathbb{R}^2 \times \mathbb{R}_{\geq 0}$). Here, we denote $\mathbb{R}_{\geq 0} = \{x \in \mathbb{R} \mid x \geq 0\}$. See Figure 2. We will denote the set of all such *generic* points in $\mathbf{MA}(\Omega)$ by $G(\Omega)$, and, for every $p \in G(\Omega)$, define $0 < \theta(p) \leq \frac{\pi}{2}$ to be the angle between $\overline{pq_1}$ (or equivalently $\overline{pq_2}$) and $\mathbf{MA}(\Omega)$ at p, where q_1, q_2 are the two contact points (Figure 2 (a)). We also define $\alpha(p) \geq 0$ to be the angle between the plane $\mathbb{R}^2$ (that is, $\mathbb{R}^2 \times \{0\}$ in $\mathbb{R}^2 \times \mathbb{R}_{\geq 0}$) and $\mathbf{MAT}(\Omega)$ at P (Figure 2 (b)). It is easy to see that

$$\cos\theta(p) = \tan\alpha(p), \tag{1}$$

for every $p \in G(\Omega)$. Note that, for every $p \in G(\Omega)$, we have $0 \leq \alpha(p) < 1$, since $0 \leq \theta(p) < \frac{\pi}{2}$.

Now, for every normal domain Ω, we define

$$\begin{aligned}
\theta_\Omega &= \inf\{\theta(p) : p \in G(\Omega)\}, \\
\alpha_\Omega &= \sup\{\alpha(p) : p \in G(\Omega)\}.
\end{aligned}$$

Then, from (1), we have

$$\cos\theta_\Omega = \tan\alpha_\Omega. \tag{2}$$

Note that $0 \leq \theta_\Omega \leq \frac{\pi}{2}$ and $0 \leq \alpha_\Omega \leq \frac{\pi}{4}$. We also define

$$\rho_\Omega = \min\{r : (p, r) \in \mathbf{MAT}(\Omega)\},$$

3

that is, ρ_Ω is the smallest radius of the maximal balls contained in Ω.

We call an end point of **MA** (or **MAT**) a 1-*prong point*. There are exactly three kinds of the 1-prong points in **MA**, which are depicted in Figure 3; Type (a) is the center of a maximal circle with only one contact point at which the circle osculates the boundary. Type (b) is a sharp corner. Type (c) is a 1-prong point with a contact arc. It is easy to see that $\theta_\Omega = 0$, if and only if **MA**(Ω) has a 1-prong point of the type (a), and $\rho_\Omega = 0$, if and only if **MA**(Ω) has a 1-prong point of the type (b).

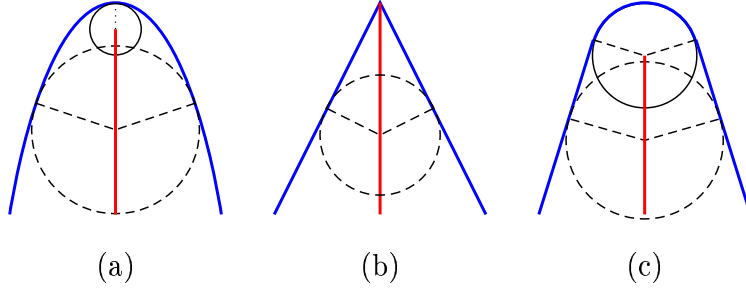(a)   (b)   (c)

Figure 3: Three types of 1-prong points

We call a normal domain Ω *injective*, if $\theta_\Omega > 0$ and $\rho_\Omega > 0$, and *weakly injective*, if $\theta_\Omega > 0$. Thus, Ω is injective, if and only if every end point of **MA**(Ω) is of the type (c), and it is weakly injective, if and only if **MA**(Ω) does not have the end points of the type (a). Note that a weakly injective domain may have a sharp corner (*i.e.*, the type (b)), while an injective domain may not.

For more details on the properties of the medial axis transform, see [2, 3, 7].

2.2   Hausdorff Distance : Euclidean *vs.* Hyperbolic

Although sometimes it might be misleading [5], the Hausdorff distance is a natural device to measure the difference between two shapes. Let A and B be two (compact) sets in $\mathbb{R}^2$. The *one-sided Hausdorff distance* of A with respect to B, $\mathcal{H}(A|B)$, is defined by

$$\mathcal{H}(A|B) = \max_{p \in A} d(p, B),$$

where $d(\cdot, \cdot)$ is the usual Euclidean distance. The *(two-sided) Hausdorff distance* between A and B, $\mathcal{H}(A, B)$, is defined by

$$\mathcal{H}(A, B) = \max \{\mathcal{H}(A|B), \mathcal{H}(B|A)\}.$$

4

Note that, whereas the two-sided Hausdorff distance measures the difference between two sets, the one-sided Hausdorff distance measures how approximately one set is contained in another set.

Though the Hausdorff distance is intuitively appealing, it cannot capture well the seemingly unstable behaviour of **MAT** under the perturbation. Recently, there has been the introduction of a new measure called the *hyperbolic Hausdorff distance*, so that **MAT** (and **MA**) becomes stable, if the difference between two **MAT**s is measured by this measure [5] (See Proposition 1 below).

Let $P_1 = (p_1, r_1), P_2 = (p_2, r_2)$ be in $\mathbb{R}^2 \times \mathbb{R}_{\geq 0}$. Then the *hyperbolic distance $d_h(P_1|P_2)$ from P_1 to P_2* is defined by

$$d_h(P_1|P_2) = \max \{0, d(p_1, p_2) - (r_2 - r_1)\}. \tag{3}$$

We will need the following triangular inequality for the hyperbolic distance [5]: For any $P_1, P_2, P_3 \in \mathbb{R}^2 \times \mathbb{R}_{\geq 0}$,

$$d_h(P_1|P_3) \leq d_h(P_1|P_2) + d_h(P_2|P_3). \tag{4}$$

Let M_1, M_2 be compact sets in $\mathbb{R}^2 \times \mathbb{R}_{\geq 0}$. Then the *one-sided hyperbolic Hausdorff distance $\mathcal{H}_h(M_1|M_2)$ of M_1* with respect to M_2 is defined by

$$\mathcal{H}_h(M_1|M_2) = \max_{P_1 \in M_1} \left\{ \min_{P_2 \in M_2} d_h(P_1|P_2) \right\}, \tag{5}$$

and the *(two-sided) hyperbolic Hausdorff distance* between M_1 and M_2 is defined by

$$\mathcal{H}_h(M_1, M_2) = \max \{\mathcal{H}_h(M_1|M_2), \mathcal{H}_h(M_2|M_1)\}. \tag{6}$$

Proposition 1. ([5]) *For any normal domains Ω_1 and Ω_2, we have*

$$
\begin{aligned}
\max \{\mathcal{H}(\Omega_1, \Omega_2), \mathcal{H}(\partial\Omega_1, \partial\Omega_2)\} &\leq \mathcal{H}_h(\mathbf{MAT}(\Omega_1), \mathbf{MAT}(\Omega_2)), \\
\mathcal{H}_h(\mathbf{MAT}(\Omega_1), \mathbf{MAT}(\Omega_2)) &\leq 3 \cdot \max \{\mathcal{H}(\Omega_1, \Omega_2), \mathcal{H}(\partial\Omega_1, \partial\Omega_2)\}.
\end{aligned}
$$

In this paper, we will use the second inequality to extend the result for the injective domains in [4] to a result for the weakly injective domains.

3 Infinitesimal Perturbation of Injective Domain

Before we prove our result on the weakly injective domains, we first review the previous result for the injective domains.

Proposition 2. ([4]) *Let Ω be an injective domain, and let Ω' be a normal domain with $\max\{\mathcal{H}(\Omega, \Omega'), \mathcal{H}(\partial\Omega, \partial\Omega')\} \leq \epsilon$, where $\epsilon < \min\{\rho_\Omega \tan^2(\theta_\Omega/2), \rho_\Omega/2\}$. Then we have*

$$
\begin{aligned}
\mathcal{H}(\mathbf{MA}(\Omega)|\mathbf{MA}(\Omega')) &\leq \eta, \\
\mathcal{H}(\mathbf{MAT}(\Omega)|\mathbf{MAT}(\Omega')) &\leq \sqrt{\eta^2 + \{\epsilon + \eta\}^2},
\end{aligned}
$$

where

$$
\eta = \frac{\rho_\Omega \cdot \epsilon}{\rho_\Omega \sin^2(\theta_\Omega/2) - \epsilon \cos^2(\theta_\Omega/2)}.
$$

Note that this result applies only to the small perturbation of the injective domain, *i.e.*, when $\epsilon < \min\{\rho_\Omega \tan^2(\theta_\Omega/2), \rho_\Omega/2\}$. By using the Taylor expansion, the following infinitesimally *linear* bound of the one-sided Hausdorff distance for injective domains can easily be deduced:

Corollary 1. (Infinitesimal Perturbation of Injective Domain) *Let Ω be an injective domain. Then we have*

$$
\begin{aligned}
\mathcal{H}(\mathbf{MA}(\Omega)|\mathbf{MA}(\Omega')) &\leq \frac{2}{1 - \cos\theta_\Omega} \cdot \epsilon + o(\epsilon), \\
\mathcal{H}(\mathbf{MAT}(\Omega)|\mathbf{MAT}(\Omega')) &\leq \frac{\sqrt{4 + (3 - \cos\theta_\Omega)^2}}{1 - \cos\theta_\Omega} \cdot \epsilon + o(\epsilon),
\end{aligned}
$$

for every normal domain Ω' such that $\max\{\mathcal{H}(\Omega, \Omega'), \mathcal{H}(\partial\Omega, \partial\Omega')\} \leq \epsilon$.

4 Perturbation of Weakly Injective Domain

Let $P_i = (p_i, r_i)$, $i = 1, 2$ be two different points in $\mathbb{R}^2 \times \mathbb{R}_{\geq 0}$. We will denote by $-\frac{\pi}{2} \leq \alpha(P_1, P_2) \leq \frac{\pi}{2}$ the angle from $\mathbb{R}^2 \times \{0\}$ to $\overrightarrow{P_1 P_2}$ in $\mathbb{R}^2 \times \mathbb{R}_{\geq 0}$, *i.e.*, $\alpha(P_1, P_2)$ is given by

$$
\sin\alpha(P_1, P_2) = \overrightarrow{e_r} \cdot \frac{\overrightarrow{P_1 P_2}}{d(P_1, P_2)},
$$

where $\overrightarrow{e_r} = ((0, 0), 1)$. See Figure 4.

Suppose $|\alpha(P_1, P_2)| < \frac{\pi}{4}$, which, in fact, is always true when $P_1, P_2 \in \mathbf{MAT}(\Omega)$ for some normal domain Ω. From (3), it is clear that

$$
d_h(P_1|P_2) = \{\cos\alpha(P_1, P_2) - \sin\alpha(P_1, P_2)\} \cdot d(P_1, P_2).
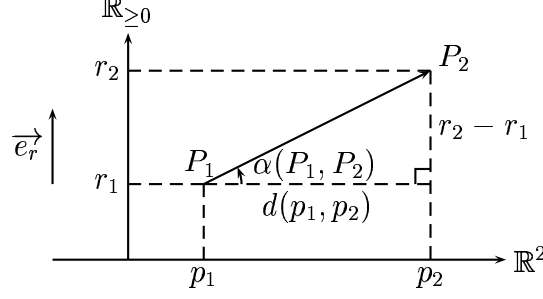$$

6

Figure 4: Two points in $\mathbb{R}^2 \times \mathbb{R}_{\geq 0}$

So we have

$$\frac{d(P_1, P_2)}{d_h(P_1|P_2)} = \frac{1}{\cos \alpha(P_1, P_2) - \sin \alpha(P_1, P_2)}. \qquad (7)$$

We will show that, both infinitesimally and globally, the one-sided Hausdorff distance of **MAT** (and **MA**) of a weakly injective domain is bounded linearly by the magnitude of the perturbation. For these results, we need the following two key lemmas, which will be proved in Appendices.

Lemma 1. *Let Ω be a weakly injective domain. Then we have*

$$\sup \left\{ \frac{d(P_1, P_2)}{d_h(P_1|P_2)} : P_1 \neq P_2 \in \mathbf{MAT}(\Omega) \right\} < \infty,$$

and

$$\sup \left\{ \frac{d(P_1, P_2)}{d_h(P_1|P_2)} : P_1 \neq P_2 \in \mathbf{MAT}(\Omega), d_h(P_1|P_2) \leq \epsilon \right\}$$

$$\leq \frac{\sqrt{1 + \cos^2 \theta_\Omega}}{1 - \cos \theta_\Omega} + o(1).$$

Lemma 2. *Let P_1, P_2, P_3 be in $\mathbb{R}^2 \times \mathbb{R}_{\geq 0}$. Suppose $d_h(P_1|P_2) \leq \epsilon$ and $d_h(P_2|P_3) \leq \epsilon$ for some $\epsilon \geq 0$. Then we have*

$$d(P_1, P_2) \leq d(P_1, P_3) + \epsilon.$$

Define a function $g : (0, \pi/2] \to \mathbb{R}$ by

$$g(\theta) = 3 \left(1 + \frac{2\sqrt{1 + \cos^2 \theta}}{1 - \cos \theta} \right).$$

7

See Figure 5 for the graph of g. Also, by Lemma 1, we can define

$$k_\Omega = 3\left(1 + 2R_\Omega\right),$$

for every weakly injective domain Ω, where

$$R_\Omega = \sup\left\{\frac{d(P_1, P_2)}{d_h(P_1|P_2)} : P_1 \neq P_2 \in \mathbf{MAT}(\Omega)\right\}.$$

Theorem 1. (Infinitesimal Perturbation of Weakly Injective Domain) *Let Ω be a weakly injective domain. Then we have*

$$\begin{aligned}
\mathcal{H}(\mathbf{MAT}(\Omega)|\mathbf{MAT}(\Omega')) &\leq g(\theta_\Omega) \cdot \epsilon + o(\epsilon), \\
\mathcal{H}(\mathbf{MA}(\Omega)|\mathbf{MA}(\Omega')) &\leq g(\theta_\Omega) \cdot \epsilon + o(\epsilon),
\end{aligned}$$

for every $\epsilon \geq 0$, and for every normal domain Ω' such that $\max\{\mathcal{H}(\Omega, \Omega'), \mathcal{H}(\partial\Omega, \partial\Omega')\} \leq \epsilon$.

Theorem 2. (Global Perturbation of Weakly Injective Domain) *Let Ω be a weakly injective domain. Then we have*

$$\begin{aligned}
\mathcal{H}(\mathbf{MAT}(\Omega)|\mathbf{MAT}(\Omega')) &\leq k_\Omega \cdot \epsilon, \\
\mathcal{H}(\mathbf{MA}(\Omega)|\mathbf{MA}(\Omega')) &\leq k_\Omega \cdot \epsilon,
\end{aligned}$$

for every $\epsilon \geq 0$, and for every normal domain Ω' such that $\max\{\mathcal{H}(\Omega, \Omega'), \mathcal{H}(\partial\Omega, \partial\Omega')\} \leq \epsilon$.

Proof of Theorems 1 and 2. First, note that $\mathcal{H}(\mathbf{MA}(\Omega)|\mathbf{MA}(\Omega')) \leq \mathcal{H}(\mathbf{MAT}(\Omega)|\mathbf{MAT}(\Omega'))$. So we only need to bound the latter. Let $P \in \mathbf{MAT}(\Omega)$. By Proposition 1, we have $\mathcal{H}_h(\mathbf{MAT}(\Omega), \mathbf{MAT}(\Omega')) \leq 3\epsilon$. So by (5) and (6), there exists $P' \in \mathbf{MAT}(\Omega')$ such that $d_h(P|P') \leq 3\epsilon$, and, again, there exists $P'' \in \mathbf{MAT}(\Omega)$ such that $d_h(P'|P'') \leq 3\epsilon$. So $d_h(P|P'') \leq 6\epsilon$ by (4). From Lemma 1, we have $d(P, P'') \leq \frac{\sqrt{1+\cos^2\theta_\Omega}}{1-\cos\theta_\Omega} \cdot 6\epsilon + o(\epsilon)$ and $d(P, P'') \leq R_\Omega \cdot 6\epsilon$. So, by Lemma 2, $d(P, P') \leq 3\epsilon + \frac{\sqrt{1+\cos^2\theta_\Omega}}{1-\cos\theta_\Omega} \cdot 6\epsilon + o(\epsilon) = g(\theta_\Omega) \cdot \epsilon + o(\epsilon)$, and $d(P, P') \leq 3\epsilon + R_\Omega \cdot 6\epsilon = k_\Omega \cdot \epsilon$. Since P is taken arbitrarily in $\mathbf{MAT}(\Omega)$, these imply Theorems 1 and 2 respectively. $\square$

Example 1. *Let Ω be a weakly injective domain with a sharp corner P_1 depicted as in Figure 6. Let Ω' be the domain obtained by smoothing Ω near P_1 so that $\mathbf{MAT}(\Omega) = \overline{P_2 P_3}$. Let $P_i = (p_i, r_i)$ for $i = 1, 2, 3$. Note that*

$$\mathcal{H}(\Omega, \Omega') = \mathcal{H}(\partial\Omega, \partial\Omega') = \epsilon,$$
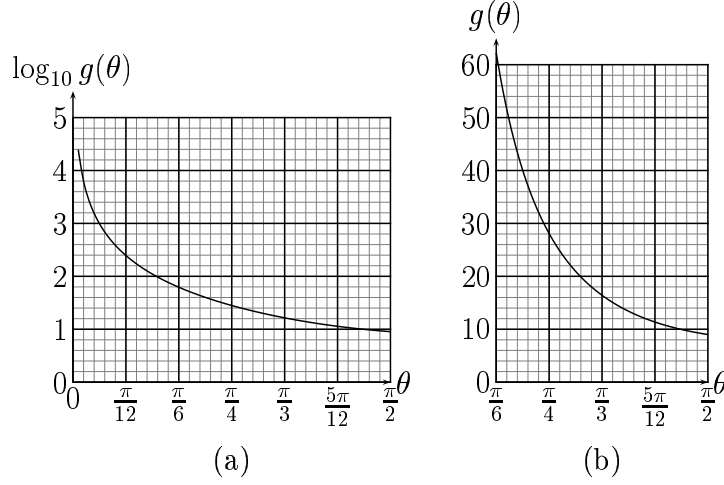
8

Figure 5: The graph of the coefficient function $g(\theta) = 3\left(1 + \frac{2\sqrt{1+\cos^2\theta}}{1-\cos\theta}\right)$; (a) The logarithmic graph of g on the whole interval $(0, \frac{\pi}{2}]$, (b) The (normal) graph of g on the interval $[\frac{\pi}{6}, \frac{\pi}{2}]$.

and

$$\mathcal{H}(\mathbf{MA}(\Omega)|\mathbf{MA}(\Omega')) = d(p_1, p_2) = \frac{1}{1-\cos\theta_\Omega} \cdot \epsilon,$$

$$\mathcal{H}(\mathbf{MAT}(\Omega)|\mathbf{MAT}(\Omega')) = d(P_1, P_2) = \frac{\sqrt{1+\cos^2\theta_\Omega}}{1-\cos\theta_\Omega} \cdot \epsilon.$$

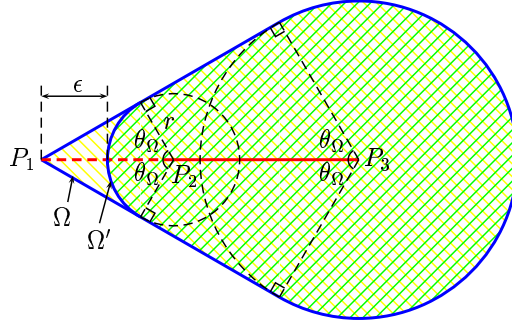

Figure 6: One-sided stability for weakly injective domain

This example shows that the factor $\frac{1}{1-\cos\theta_\Omega}$ in $g(\theta_\Omega)$, which blows up as $\theta_\Omega \to 0$, is indeed unavoidable. One important consequence is that the class

9

of the weakly injective domains is the largest possible class for which we have a linear bound for the one-sided Hausdorff distance of **MAT** (and **MA**) with respect to the perturbation.

From Lemma 1, it is easy to see that $k_\Omega \geq g(\theta_\Omega)$. The example in Figure 7 shows that the global constant k_Ω can be strictly greater than the infinitesimal constant $g(\theta_\Omega)$.
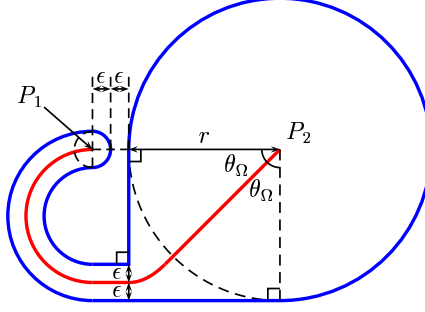

Figure 7: Global constant can differ from infinitesimal constant; Here, $\theta_\Omega = \frac{\pi}{4}$, and hence, $g(\theta_\Omega) = 3\left(1 + 2\sqrt{3}(1 + \sqrt{2})\right) = 28.089243\cdots$. But $k_\Omega = 3 + 6 \cdot \frac{d(P_1, P_2)}{d_h(P_1|P_2)} = 3 + 6 \cdot \frac{\sqrt{(r+2\epsilon)^2 + (r-\epsilon)^2}}{3\epsilon} \to \infty$ as $\epsilon \to 0$.

5   The Essential Part of the MAT : Relation to Pruning

Theorem 1 together with Example 1 says that the angle θ_Ω is an important quantity reflecting the degree of the "detailed-ness" of a domain Ω. The smaller θ_Ω becomes, the finer approximation, that is, the smaller $\max\{\mathcal{H}(\Omega, \Omega'),$ $\mathcal{H}(\partial\Omega, \partial\Omega')\}$ is needed for **MAT**(Ω') and **MA**(Ω') of another domain Ω' to contain (approximately) **MAT**(Ω) and **MA**(Ω) respectively.

Suppose we perturb a weakly injective domain with domains which are also weakly injective. In this case, **MAT** and **MA** become stable under the "two-sided" Hausdorff distance. In particular, we have the following corollary:

Corollary 2. (Approximation by Weakly Injective Domains) *Let Ω be a normal domain, and let Ω_1 and Ω_2 be two weakly injective domains such that* $\max\{\mathcal{H}(\Omega_i, \Omega), \mathcal{H}(\partial\Omega_i, \partial\Omega)\} \leq \epsilon$ *for $i = 1, 2$. Let $\theta = \min\{\theta_{\Omega_1}, \theta_{\Omega_2}\}$.*

Then we have

$$\mathcal{H}\left(\mathbf{MAT}(\Omega_1), \mathbf{MAT}(\Omega_2)\right) < 2g(\theta) \cdot \epsilon + o(\epsilon),$$
$$\mathcal{H}\left(\mathbf{MA}(\Omega_1), \mathbf{MA}(\Omega_2)\right) < 2g(\theta) \cdot \epsilon + o(\epsilon).$$

Proof. This follows by applying Theorem 1 symmetrically to Ω_1 and Ω_2, and from the fact that $\mathcal{H}(\Omega_1, \Omega_2) \leq \mathcal{H}(\Omega_1, \Omega) + \mathcal{H}(\Omega_2, \Omega) \leq 2\epsilon$, $\mathcal{H}(\partial\Omega_1, \partial\Omega_2) \leq \mathcal{H}(\partial\Omega_1, \partial\Omega) + \mathcal{H}(\partial\Omega_2, \partial\Omega) \leq 2\epsilon$. □

Thus, the effect on **MAT** and **MA** which arises from the choice of the weakly injective domains to approximate a normal domain is relatively small. So the **MAT** and the **MA** of an approximating weakly injective domain may be considered as a common part among all the other approximations with the same θ_Ω, and hence, an essential part of the original **MAT** and **MA** with the fine details determined by the value of θ_Ω. This suggests that, by approximating a given normal domain with the weakly injective domains, it is possible to extract approximately the most essential part of the original **MAT** and **MA**, which is the main objective of the existing pruning methods.

6   Illustrating Examples

Now we will consider a few examples, and calculate explicitly the constants θ_Ω, $g(\theta_\Omega)$ and k_Ω for each of them. Keep in mind that k_Ω is determined by the supremum of the value $\frac{d(P_1, P_2)}{d_h(P_1|P_2)}$, and hence from (7), by that of the angle $\alpha(P_1, P_2)$, for $P_1 \neq P_2$ in $\mathbf{MAT}(\Omega)$.

Example 2. *Consider an equilateral triangle and a star-shaped domain depicted respectively as in Figure 8 (a) and (b). Note that $\theta_\Omega = \frac{\pi}{3}$ for (a), and $\theta_\Omega = \frac{\pi}{5}$ for (b). So $g(\theta_\Omega) = 3(1 + 2\sqrt{5}) = 16.416408\cdots$ for (a), and $g(\theta_\Omega) = 43.410203\cdots$ for (b). In both cases, it is easy to see that $k_\Omega = g(\theta)$.*

Example 3. *Consider the tubular domains with (a) constant width, and (b) with increasing width, which are depicted as in Figure 9. Their **MAT**s are parametrized respectively by*

$$P(t) = ((R\sin t, R - R\cos t), r),$$
$$P(t) = ((R\sin t, R - R\cos t), r + at),$$

for $t \in [0, \frac{\pi}{2}]$. Here, it is assumed that $R \gg r \gg a > 0$. For (a), it easy easy to see that $\theta_\Omega = \frac{\pi}{2}$, and $k_\Omega = g(\theta_\Omega) = 9$. For (b), we have $\theta_\Omega = \arccos\frac{a}{R}$,
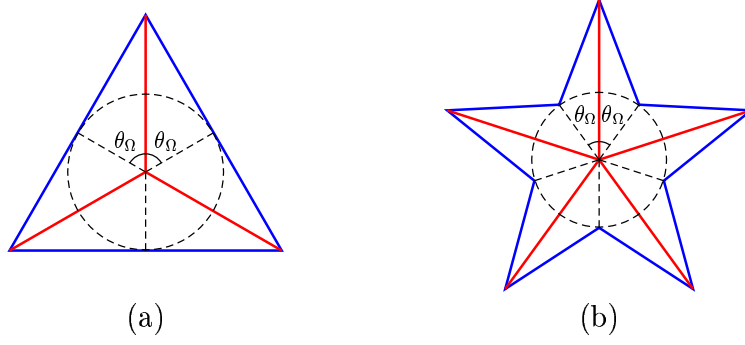
11

Figure 8: (a) Equilateral triangle; $\theta_\Omega = \frac{\pi}{3}$, (b) five-sided star; $\theta_\Omega = \frac{\pi}{5}$. For both cases, we have $k_\Omega = g(\theta_\Omega)$.

and so

$$g(\theta_\Omega) = 3 + 6 \cdot \frac{\sqrt{1 + \left(\frac{a}{R}\right)^2}}{1 - \frac{a}{R}}.$$

But

$$k_\Omega = 3 + 6 \cdot \frac{d(O,P)}{d_h(O|P)} = 3 + 6 \cdot \frac{\sqrt{1 + \left(\frac{\pi}{2\sqrt{2}} \cdot \frac{a}{R}\right)^2}}{1 - \frac{\pi}{2\sqrt{2}} \cdot \frac{a}{R}}.$$

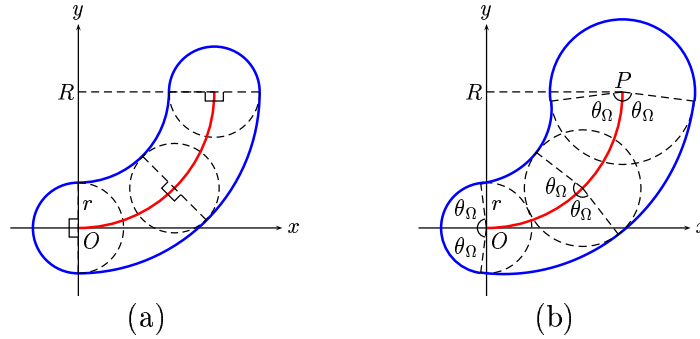*Thus, it is easy to see that $k_\Omega > g(\theta_\Omega)$.*

Figure 9: (a) Tube with constant width; $\theta_\Omega = \frac{\pi}{2}$ and $k_\Omega = g(\theta_\Omega) = 9$. (b) Tube whose width increases at a constant ratio $a > 0$; $\theta_\Omega = \arccos \frac{a}{R}$ and $k_\Omega > g(\theta_\Omega)$.

Example 4. *Consider the rectangular domains with constant widths depicted as in Figure 10. Note that $\theta_\Omega = \frac{\pi}{4}$ for all cases. It is also easy to see that*

12

$k_\Omega = g(\theta_\Omega) = 3\left(1 + 2\sqrt{3}(1 + \sqrt{2})\right) = 28.089243\cdots$ *for all cases. Note that the same result applies to the domain in Figure 11.*
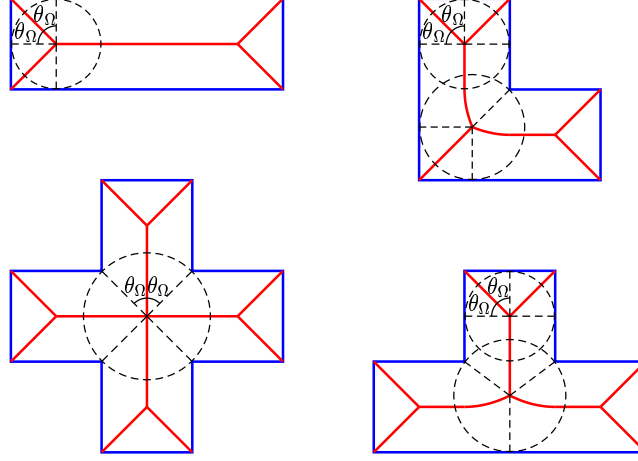

Figure 10: Rectangular domains with constant widths; For all cases, we have $\theta_\Omega = \frac{\pi}{4}$ and $k_\Omega = g(\theta_\Omega) = 3\left(1 + 2\sqrt{3}(1 + \sqrt{2})\right) = 28.089243\cdots$.
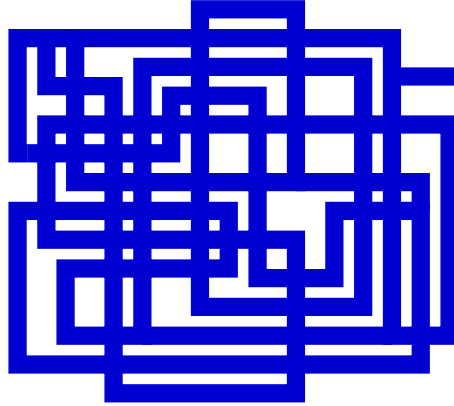

Figure 11: Complex tubular shape with constant width; here, we also have $\theta_\Omega = \frac{\pi}{4}$ and $k_\Omega = g(\theta_\Omega) = 3\left(1 + 2\sqrt{3}(1 + \sqrt{2})\right) = 28.089243\cdots$.

Appendix A. Proof of Lemma 1

First, note that the first inequality comes immediately from the second one, since the set $\mathbf{MAT}(\Omega) \times \mathbf{MAT}(\Omega) \backslash \{(P_1, P_2) \mid P_1, P_2 \in \mathbf{MAT}(\Omega), d_h(P_1|P_2) < \epsilon\}$

13

is compact for any $\epsilon > 0$, and the function $\frac{d(P_1,P_2)}{d_h(P_1|P_2)}$ is continuous on it. Let

$$A_\epsilon = \sup \{\alpha(P_1, P_2) : P_1 \neq P_2 \in \mathbf{MAT}(\Omega), d_h(P_1|P_2) \leq \epsilon\}.$$

Note that $|A_\epsilon| \leq \frac{\pi}{4}$ for any $\epsilon > 0$, since $|\alpha(P_1, P_2)| < \frac{\pi}{4}$ for any $P_1 \neq P_2 \in \mathbf{MAT}(\Omega)$. We will show that $\limsup_{\epsilon \to 0} A_\epsilon \leq \alpha_\Omega$. Note that $\alpha_\Omega < \frac{\pi}{4}$ by (2), since Ω is weakly injective. Suppose $\limsup_{\epsilon \to 0} A_\epsilon > \alpha_\Omega$. Then there exist sequences $\{P_1^m\}$, $\{P_2^m\}$ in $\mathbf{MAT}(\Omega)$ such that $P_1^m \neq P_2^m$, $d_h(P_1^m|P_2^m) \leq 1/2^m$, and $\lim_{m \to \infty} \alpha(P_1^m, P_2^m) > \alpha_\Omega$. Since $\mathbf{MAT}(\Omega)$ is compact, we can assume $d(P_1^m, P_1) \to 0$ and $d(P_2^m, P_2) \to 0$ as $m \to \infty$ for some $P_1, P_2 \in \mathbf{MAT}(\Omega)$. Since $d_h(P_1^m|P_2^m) \to 0$ as $m \to \infty$, it follows that $P_1 = P_2$, which we denote $P = (p, r)$.

Note that, around every point in $\mathbf{MAT}$ (including, of course, the generic ones) of a normal domain, $\mathbf{MAT}$ consists of n C^1 curves (called prongs) emanating from the point for some $n \geq 1$ [3]. We call such point an n-prong point. See Figure 12. Now P is an n-prong for some $n \geq 1$. Let $\mathcal{P}_1, \cdots, \mathcal{P}_n$ be the prongs of $\mathbf{MAT}(\Omega)$ around P. Since each of the prongs is C^1 at P, we can define $\alpha_j = \lim_{Q \to P, Q \in \mathcal{P}_j} \alpha(P, Q)$ for $j = 1, \cdots, n$. It is easy to see that $|\alpha_j| \leq \alpha_\Omega$ for $j = 1, \cdots, n$.
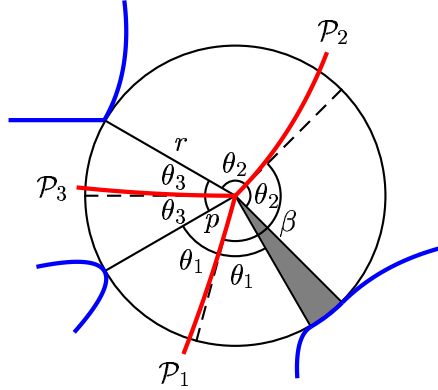

Figure 12: Local geometry of $\mathbf{MAT}$ around an n-prong point

With no loss of generality, we can assume that, for each $i = 1, 2$, the sequence $\{P_i^m\}$ lies only on one prong of $\mathbf{MAT}(\Omega)$ around P. If the two sequences $\{P_1^m\}$ and $\{P_2^m\}$ are on the same prong, say $\mathcal{P}_1$, then it is easy to see that $\lim_{m \to \infty} |\alpha(P_1^m, P_2^m)| = |\alpha_1| \leq \alpha_\Omega$, which contradicts the assumption. So we can assume with no loss of generality that $\{P_i^m\}$ is on $\mathcal{P}_i$ for $i = 1, 2$.

Parametrize $\mathcal{P}_1$ and $\mathcal{P}_2$ by $P_1(t_1) = (p_1(t_1), r_1(t_1))$, $t_1 \geq 0$ and $P_2(t_2) = (p_2(t_2), r_2(t_2))$, $t_2 \geq 0$ respectively so that $|p_i'| \equiv 1$ and $P_i(0) = P$ for $i = 1, 2$.

Then, within the first order approximation, we have

$$\tan \alpha \left(P_1(t_1), P_2(t_2) \right) = \frac{t_2 \tan \alpha_2 - t_1 \tan \alpha_1}{\sqrt{t_1^2 + t_2^2 - 2t_1 t_2 \cos \beta}}, \tag{8}$$

for $t_1, t_2 > 0$, where $0 < \beta \le \pi$ is the angle between $p_1'(0)$ and $p_2'(0)$. Let $t_1 = t$ and $t_2 = kt$ for $k > 0$. Then the right side of (8) becomes

$$\frac{k \tan \alpha_2 - \tan \alpha_1}{\sqrt{k^2 + 1 - 2k \cos \beta}}. \tag{9}$$

Note that $\beta \ge \theta_1 + \theta_2$, where $\cos \theta_i = -\tan \alpha_i$, $0 < \theta_i < \pi$ for $i = 1, 2$ (See Figure 12). So $\cos \beta \le \cos(\theta_1 + \theta_2) = \cos \theta_1 \cos \theta_2 - \sin \theta_1 \sin \theta_2 \le \cos \theta_1 \cos \theta_2 = \tan \alpha_1 \tan \alpha_2$. So (9) is less than

$$\frac{k \tan \alpha_2 - \tan \alpha_1}{\sqrt{k^2 + 1 - 2k \tan \alpha_1 \tan a_2}}. \tag{10}$$

Now it is easy to see that (10) is less than $\max \{ |\tan \alpha_1|, |\tan \alpha_2| \} \le \tan \alpha_\Omega$ for every $k > 0$. This implies that $\lim_{m \to \infty} \alpha(P_1^m, P_2^m) \le \alpha_\Omega$, since $\{P_i^m\}$ is on $\mathcal{P}_i$, and is approaching to P for $i = 1, 2$. Thus we have a contradiction to the assumption, and hence, we conclude that $\limsup_{\epsilon \to 0} A_\epsilon \le \alpha_\Omega$.

Thus, from (7), we have

$$\sup \left\{ \frac{d(P_1, P_2)}{d_h(P_1 | P_2)} : P_1 \ne P_2 \in \mathbf{MAT}(\Omega), d_h(P_1 | P_2) \le \epsilon \right\}$$

$$\le \frac{1}{\cos A_\epsilon - \sin A_\epsilon} \le \frac{1}{\cos \alpha_\Omega - \sin \alpha_\Omega} + o(1).$$

This shows the second inequality, since, from (2), we have

$$\frac{1}{\cos \alpha_\Omega - \sin \alpha_\Omega} = \frac{\sqrt{1 + \cos^2 \theta_\Omega}}{1 - \cos \theta_\Omega}.$$

Appendix B. Proof of Lemma 2

From the assumptions and (3), we have

$$d(p_1, p_2) \le r_2 - r_1 + \epsilon, \tag{11}$$
$$d(p_2, p_3) \le r_3 - r_2 + \epsilon. \tag{12}$$

Let $D_2 = d(P_1, P_2)$ and $D_3 = d(P_1, P_3)$. Suppose the result does not hold, i.e.,

$$D_2 > D_3 + \epsilon. \tag{13}$$

15

Note that $D_2 > \epsilon$, and hence $D_2 > 0$. Choose $-\frac{\pi}{2} \leq \theta_2, \theta_3 \leq \frac{\pi}{2}$ such that

$$d(p_1, p_2) = D_2 \cos \theta_2, \qquad r_2 - r_1 = D_2 \sin \theta_2,$$
$$d(p_1, p_3) = D_3 \cos \theta_3, \qquad r_3 - r_1 = D_3 \sin \theta_3.$$

Note that $\cos \theta_2 \geq 0$. From (11), we have

$$D_2(\cos \theta_2 - \sin \theta_2) \leq \epsilon. \tag{14}$$

Since $D_2 > \epsilon$, we have $\cos \theta_2 - \sin \theta_2 < 1$ from (14), which implies that $\sin \theta_2 > 0$. So

$$\cos \theta_2 + \sin \theta_2 > 0. \tag{15}$$

Note that $d(p_2, p_3) \geq |d(p_1, p_2) - d(p_1, p_3)|$ by the triangular inequality for the Euclidean distance. So from (12), we have

$$d(p_1, p_2) - d(p_1, p_3) \leq (r_3 - r_1) - (r_2 - r_1) + \epsilon,$$
$$d(p_1, p_3) - d(p_1, p_2) \leq (r_3 - r_1) - (r_2 - r_1) + \epsilon,$$

which are equivalent respectively to

$$D_2(\cos \theta_2 + \sin \theta_2) \leq D_3(\cos \theta_3 + \sin \theta_3) + \epsilon, \tag{16}$$
$$D_2(\cos \theta_2 - \sin \theta_2) \geq D_3(\cos \theta_3 - \sin \theta_3) - \epsilon. \tag{17}$$

From (14), (15), (16), and (17), we have

$$0 < D_2(\cos \theta_2 + \sin \theta_2) \leq D_3(\cos \theta_3 + \sin \theta_3) + \epsilon,$$
$$D_3(\cos \theta_3 - \sin \theta_3) - \epsilon \leq D_2(\cos \theta_2 - \sin \theta_2) \leq \epsilon,$$

and so

$$D_2^2(\cos \theta_2 + \sin \theta_2)^2 \leq \{D_3(\cos \theta_3 + \sin \theta_3) + \epsilon\}^2,$$
$$D_2^2(\cos \theta_2 - \sin \theta_2)^2 \leq \max \{\epsilon^2, \{D_3(\cos \theta_3 - \sin \theta_3) - \epsilon\}^2\}.$$

By adding the above two inequalities, we get

$$2D_2^2 \leq \{D_3(\cos \theta_3 + \sin \theta_3) + \epsilon\}^2$$
$$+ \max \{\epsilon^2, \{D_3(\cos \theta_3 - \sin \theta_3) - \epsilon\}^2\}. \tag{18}$$

If $D_3 = 0$, then it follows that $D_2 \leq \epsilon$, contradicting (13). So we assume $D_3 > 0$. Now from (18) and (13), we have

$$2(D_3 + \epsilon)^2 < \{D_3(\cos \theta_3 + \sin \theta_3) + \epsilon\}^2$$
$$+ \max \{\epsilon^2, \{D_3(\cos \theta_3 - \sin \theta_3) - \epsilon\}^2\}. \tag{19}$$

16

Suppose $|D_3(\cos\theta_3 - \sin\theta_3) - \epsilon| \leq \epsilon$. Then (19) becomes

$$
\begin{aligned}
2(D_3 + \epsilon)^2 \;&<\; \{D_3(\cos\theta_3 + \sin\theta_3) + \epsilon\}^2 + \epsilon^2 \\
&\leq\; \left(\sqrt{2}D_3 + \epsilon\right)^2 + \epsilon^2,
\end{aligned}
$$

which reduces to the contradiction that $\sqrt{2} < 1$. So we must have

$$|D_3(\cos\theta_3 - \sin\theta_3) - \epsilon| > \epsilon.$$

Now (19) becomes

$$
\begin{aligned}
2(D_3 + \epsilon)^2 \;&<\; \{D_3(\cos\theta_3 + \sin\theta_3) + \epsilon\}^2 \\
&\quad + \{D_3(\cos\theta_3 - \sin\theta_3) - \epsilon\}^2 \\
&=\; 2D_3^2 + 4\epsilon\sin\theta_3 D_3 + 2\epsilon^2,
\end{aligned}
$$

which reduces to the contradiction $1 < \sin\theta_3$. Thus we conclude that the assumption (13) is false, and hence, we have the desired result.

References

[1] J. August, K. Siddiqi and S. W. Zucker, "Ligature instabilities and the perceptual organization of shape," *Computer Vision and Image Understanding*, vol. 76, no. 3, pp. 231–243, Dec. 1999.

[2] H. Blum, "A transformation for extracting new descriptors of shape," *Proc. Symp. Models for the Perception of Speech and Visual Form* (W.W. Dunn, ed.), MIT Press, Cambridge, MA, pp. 362–380, 1967.

[3] H. I. Choi, S. W. Choi and H. P. Moon, "Mathematical theory of medial axis transform," *Pacific J. Math.*, vol. 181, no. 1, pp. 57–88, Nov. 1997.

[4] S. W. Choi and S.-W. Lee, "Stability analysis of medial axis transform," *Proc. 15th ICPR*, (Barcelona, Spain), vol 3, pp. 139–142, Sept. 2000.

[5] S. W. Choi and H.-P. Seidel, "Hyperbolic Hausdorff distance for medial axis transform," Research Report, MPI-I-2000-4-003, 2000.

[6] M. P. Deseilligny, G. Stamon and C. Y. Suen, "Veinerization: A new shape descriptor for flexible skeletonization," *IEEE Trans. PAMI*, vol. 20, no. 5, pp. 505–521, May 1998.

[7] P. J. Giblin and B. B. Kimia, "On the local form and transitions of symmetry sets, medial axes, and shocks," *Proc. 7th ICCV*, (Kerkyra, Greece), pp. 385–391, Sept. 1999.

[8] F. Mokhtarian and A. K. Mackworth, "A theory of multiscale, curvature-based shape representation for planar curves," *IEEE Trans. PAMI*, vol. 14, no. 8, pp. 789–805, Aug. 1992.

[9] U. Montanari, "A method for obtaining skeletons using a quasi-Euclidean distance," *J. of the ACM*, vol. 18, pp. 600–624, 1968.

[10] D. Shaked and A. M. Bruckstein, "Pruning medial axes," *Computer Vision and Image Understanding*, vol. 69, no. 2, pp. 156–169, Feb. 1998.

INFORMATIK

Below you find a list of the most recent technical reports of the Max-Planck-Institut für Informatik. They are available by anonymous ftp from `ftp.mpi-sb.mpg.de` under the directory `pub/papers/reports`. Most of the reports are also accessible via WWW using the URL `http://www.mpi-sb.mpg.de`. If you have any questions concerning ftp or WWW access, please contact `reports@mpi-sb.mpg.de`. Paper copies (which are not necessarily free of charge) can be ordered either by regular mail or by e-mail at the address below.

Max-Planck-Institut für Informatik
Library
attn. Anja Becker
Stuhlsatzenhausweg 85
66123 Saarbrücken
GERMANY
e-mail: `library@mpi-sb.mpg.de`

MPI-I-2001-4-003	K. Daubert, W. Heidrich, J. Kautz, J. Dischler, H. Seidel	Efficient Light Transport Using Precomputed Visibility
MPI-I-2001-4-002	H.P.A. Lensch, J. Kautz, M. Goesele, H. Seidel	A Framework for the Acquisition, Processing, Transmission, and Interactive Display of High Quality 3D Models on the Web
MPI-I-2001-4-001	H.P.A. Lensch, J. Kautz, M.G. Goesele, W. Heidrich, H. Seidel	Image-Based Reconstruction of Spatially Varying Materials
MPI-I-2001-2-002	P. Maier	A Set-Theoretic Framework for Assume-Guarantee Reasoning
MPI-I-2001-2-001	U. Waldmann	Superposition and Chaining for Totally Ordered Divisible Abelian Groups
MPI-I-2001-1-002	U. Meyer	Directed Single-Source Shortest-Paths in Linear Average-Case Time
MPI-I-2001-1-001	P. Krysta	Approximating Minimum Size 1,2-Connected Networks
MPI-I-2000-4-003	S.W. Choi, H. Seidel	Hyperbolic Hausdorff Distance for Medial Axis Transform
MPI-I-2000-4-002	L.P. Kobbelt, S. Bischoff, K. Kähler, R. Schneider, M. Botsch, C. Rössl, J. Vorsatz	Geometric Modeling Based on Polygonal Meshes
MPI-I-2000-4-001	J. Kautz, W. Heidrich, K. Daubert	Bump Map Shadows for OpenGL Rendering
MPI-I-2000-2-001	F. Eisenbrand	Short Vectors of Planar Lattices Via Continued Fractions
MPI-I-2000-1-005	M. Seel, K. Mehlhorn	Infimaximal Frames A Technique for Making Lines Look Like Segments
MPI-I-2000-1-004	K. Mehlhorn, S. Schirra	Generalized and improved constructive separation bound for real algebraic expressions
MPI-I-2000-1-003	P. Fatourou	Low-Contention Depth-First Scheduling of Parallel Computations with Synchronization Variables
MPI-I-2000-1-002	R. Beier, J. Sibeyn	A Powerful Heuristic for Telephone Gossiping
MPI-I-2000-1-001	E. Althaus, O. Kohlbacher, H. Lenhof, P. Müller	A branch and cut algorithm for the optimal solution of the side-chain placement problem
MPI-I-1999-4-001	J. Haber, H. Seidel	A Framework for Evaluating the Quality of Lossy Image Compression
MPI-I-1999-3-005	T.A. Henzinger, J. Raskin, P. Schobbens	Axioms for Real-Time Logics
MPI-I-1999-3-004	J. Raskin, P. Schobbens	Proving a conjecture of Andreka on temporal logic
MPI-I-1999-3-003	T.A. Henzinger, J. Raskin, P. Schobbens	Fully Decidable Logics, Automata and Classical Theories for Defining Regular Real-Time Languages

MPI-I-1999-3-002	J. Raskin, P. Schobbens	The Logic of Event Clocks
MPI-I-1999-3-001	S. Vorobyov	New Lower Bounds for the Expressiveness and the Higher-Order Matching Problem in the Simply Typed Lambda Calculus
MPI-I-1999-2-008	A. Bockmayr, F. Eisenbrand	Cutting Planes and the Elementary Closure in Fixed Dimension
MPI-I-1999-2-007	G. Delzanno, J. Raskin	Symbolic Representation of Upward-closed Sets
MPI-I-1999-2-006	A. Nonnengart	A Deductive Model Checking Approach for Hybrid Systems
MPI-I-1999-2-005	J. Wu	Symmetries in Logic Programs
MPI-I-1999-2-004	V. Cortier, H. Ganzinger, F. Jacquemard, M. Veanes	Decidable fragments of simultaneous rigid reachability
MPI-I-1999-2-003	U. Waldmann	Cancellative Superposition Decides the Theory of Divisible Torsion-Free Abelian Groups
MPI-I-1999-2-001	W. Charatonik	Automata on DAG Representations of Finite Trees
MPI-I-1999-1-007	C. Burnikel, K. Mehlhorn, M. Seel	A simple way to recognize a correct Voronoi diagram of line segments
MPI-I-1999-1-006	M. Nissen	Integration of Graph Iterators into LEDA
MPI-I-1999-1-005	J.F. Sibeyn	Ultimate Parallel List Ranking ?
MPI-I-1999-1-004	M. Nissen, K. Weihe	How generic language extensions enable "open-world" desing in Java
MPI-I-1999-1-003	P. Sanders, S. Egner, J. Korst	Fast Concurrent Access to Parallel Disks
MPI-I-1999-1-002	N.P. Boghossian, O. Kohlbacher, H.-. Lenhof	BALL: Biochemical Algorithms Library
MPI-I-1999-1-001	A. Crauser, P. Ferragina	A Theoretical and Experimental Study on the Construction of Suffix Arrays in External Memory
MPI-I-98-2-018	F. Eisenbrand	A Note on the Membership Problem for the First Elementary Closure of a Polyhedron
MPI-I-98-2-017	M. Tzakova, P. Blackburn	Hybridizing Concept Languages
MPI-I-98-2-014	Y. Gurevich, M. Veanes	Partisan Corroboration, and Shifted Pairing
MPI-I-98-2-013	H. Ganzinger, F. Jacquemard, M. Veanes	Rigid Reachability
MPI-I-98-2-012	G. Delzanno, A. Podelski	Model Checking Infinite-state Systems in CLP
MPI-I-98-2-011	A. Degtyarev, A. Voronkov	Equality Reasoning in Sequent-Based Calculi
MPI-I-98-2-010	S. Ramangalahy	Strategies for Conformance Testing
MPI-I-98-2-009	S. Vorobyov	The Undecidability of the First-Order Theories of One Step Rewriting in Linear Canonical Systems
MPI-I-98-2-008	S. Vorobyov	AE-Equational theory of context unification is Co-RE-Hard
MPI-I-98-2-007	S. Vorobyov	The Most Nonelementary Theory (A Direct Lower Bound Proof)
MPI-I-98-2-006	P. Blackburn, M. Tzakova	Hybrid Languages and Temporal Logic
MPI-I-98-2-005	M. Veanes	The Relation Between Second-Order Unification and Simultaneous Rigid E-Unification
MPI-I-98-2-004	S. Vorobyov	Satisfiability of Functional+Record Subtype Constraints is NP-Hard
MPI-I-98-2-003	R.A. Schmidt	E-Unification for Subsystems of S4
MPI-I-98-2-002	F. Jacquemard, C. Meyer, C. Weidenbach	Unification in Extensions of Shallow Equational Theories
MPI-I-98-1-031	G.W. Klau, P. Mutzel	Optimal Compaction of Orthogonal Grid Drawings
MPI-I-98-1-030	H. Brönniman, L. Kettner, S. Schirra, R. Veltkamp	Applications of the Generic Programming Paradigm in the Design of CGAL
MPI-I-98-1-029	P. Mutzel, R. Weiskircher	Optimizing Over All Combinatorial Embeddings of a Planar Graph
MPI-I-98-1-028	A. Crauser, K. Mehlhorn, E. Althaus, K. Brengel, T. Buchheit, J. Keller, H. Krone, O. Lambert, R. Schulte, S. Thiel, M. Westphal, R. Wirth	On the performance of LEDA-SM